



Transient Analysis of a Micro-reactor using the DireWolf Code Suite

May 2022

Changing the World's Energy Future

Nathan Roskoff, Vefa Kucukboyaci, Alex Levinsky, Vincent M Laboure,
Jackson R Harter, Adam X Zabriskie, Lise Cecile Madeleine Charlot



INL is a U.S. Department of Energy National Laboratory operated by Battelle Energy Alliance, LLC

DISCLAIMER

This information was prepared as an account of work sponsored by an agency of the U.S. Government. Neither the U.S. Government nor any agency thereof, nor any of their employees, makes any warranty, expressed or implied, or assumes any legal liability or responsibility for the accuracy, completeness, or usefulness, of any information, apparatus, product, or process disclosed, or represents that its use would not infringe privately owned rights. References herein to any specific commercial product, process, or service by trade name, trade mark, manufacturer, or otherwise, does not necessarily constitute or imply its endorsement, recommendation, or favoring by the U.S. Government or any agency thereof. The views and opinions of authors expressed herein do not necessarily state or reflect those of the U.S. Government or any agency thereof.

Transient Analysis of a Micro-reactor using the DireWolf Code Suite

Nathan Roskoff, Vefa Kucukboyaci, Alex Levinsky, Vincent M Laboure, Jackson R Harter, Adam X Zabriskie, Lise Cecile Madeleine Charlot

May 2022

**Idaho National Laboratory
Idaho Falls, Idaho 83415**

<http://www.inl.gov>

**Prepared for the
U.S. Department of Energy
Under DOE Idaho Operations Office
Contract DE-AC07-05ID14517, DE-AC07-05ID14517**

Transient Analysis of a Micro-reactor using the DireWolf Code Suite

Nathan Roskoff¹, Vefa Kucukboyaci¹, Alex Levinsky¹, Vincent Laboure², Jackson Harter², Adam Zabriskie², and Lise Charlot²

¹Westinghouse Electric Company
1000 Westinghouse Drive
Cranberry Township, PA 16066, USA

²Idaho National Laboratory
P.O Box 1625
Idaho Falls, ID 83415-3840, USA

nathan.roskoff@westinghouse.com, kucukbvn@westinghouse.com, levinsa@westinghouse.com, vincent.laboure@inl.gov, jackson.harter@inl.gov, adam.zabriskie@inl.gov, lise.charlot@inl.gov

doi.org/10.13182/PHYSOR22-37531

ABSTRACT

Transient analyses of heat pipe micro-reactors are necessary to ensure that hypothetical accident scenarios do not comprise reactor safety. Due to its small size and reliance on heat-pipes for cooling, the micro-reactor design introduced in this paper is a tightly coupled system which requires multi-physics tools to accurately model transient events. Idaho National Laboratory's DireWolf code suite based on the MOOSE framework is tailor-built to model heat-pipe reactors. This paper demonstrates DireWolf's ability to simulate the coupled thermal-neutronics transient behavior of a heat-pipe micro-reactor. The transient events presented here include an inadvertent rotation of all control drums simultaneously and a sudden complete rotation of a single control drum. A detailed description of each event is provided along with simulation results, including time dependent power and temperature distributions, and discussion.

KEYWORDS: Direwolf, micro-reactor, multi-physics analyses

1. INTRODUCTION

A micro-reactor, specifically one cooled with heat pipes, is intrinsically a tightly coupled system. Traditional loosely coupled, single-physics models are not sufficient to accurately predict the system behavior; a true multi-physics approach is required. To this extent, Idaho National Laboratory has taken existing MOOSE-based, finite-element computational tools and packaged them into a code suite specifically tailored for heat pipe reactors, called DireWolf [1]. DireWolf includes Griffin [2] for neutronics modeling, Bison [3] for thermal-mechanical analysis, and Sockeye [4] for heat pipe modeling.

This paper will focus on the demonstration of DireWolf's capabilities to simulate various reactivity insertion events for a heat-pipe micro-reactor. These transient events include the inadvertent simultaneous rotation of all control drums at various speeds and the sudden complete rotation of a single control drum while an adjacent drum is stuck open. Only a brief introduction to the core design and codes used is presented in this paper, details can be found in the companion paper [5]. All transient calculations presented in this paper,

will be initialized using the steady-state solution presented in the companion paper. Each of the transient events will be described in detail and results, including the power and temperature distribution time evolution, will be presented and discussed along with any sensitivity studies that have been performed. Section 2 briefly introduced the micro-reactor core and DireWolf model and Sections 3 through 5 described and provide results for each of the transients analyzed.

2. MICRO-REACTOR CORE & DIREWOLF MODEL

As previously discussed, only a brief introduction to the reactor design and DireWolf model is presented here. The 6MWth core is cooled with heat pipes which run through the entire core to the power conversion system primary heat exchanger. The reactor is fueled with 19.75 wt% enriched High-Assay Low-Enriched Uranium (HALEU) in the form of Tri-structural Isotropic (TRISO) fuel compacts. The core lifetime is approximately 3 effective full power years and achieves a core average burnup of nearly 20 GWd/MTU. For this analysis fresh fuel is used. Figure 1 shows the core geometry.

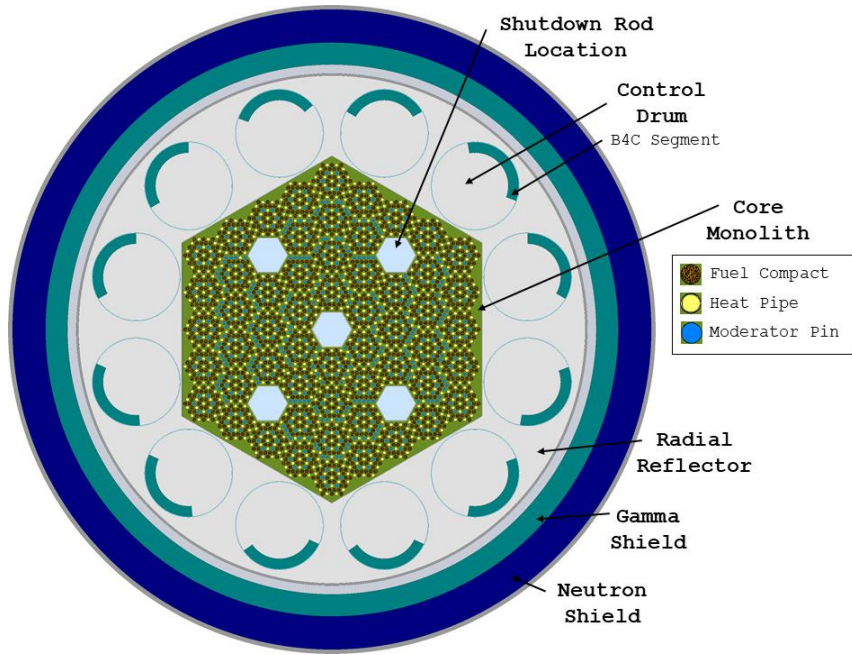


Figure 1. Micro-reactor Core Layout

As the individual physics codes of DireWolf are finite element based, generation of a mesh is required. A different mesh may be used for each physics code. For this DireWolf model both neutronics and thermal physics are performed in 3D.. Griffin (neutronics) calculations are performed on an assembly-homogenized mesh as shown in Figure 2a, using a diffusion scheme. To correct for the error associated with such a scheme and a coarse, assembly-homogenized mesh, the Super Homogenization (SPH) method, spatially restricted to the fuel regions, is used [6, 7]. No void treatment is performed as the spatial restriction of the SPH procedure to all the fuel regions can preserve the integrated leakage out of these regions [7]. In fact, the Griffin calculation can match the Serpent eigenvalues and assembly powers at state points. Between state points, the Griffin control drum rotation treatment [8] is applied to avoid cusping effects and match the Serpent critical angle within a few degrees. Note that pin-power reconstruction is not currently used, the assembly-averaged power is smeared over all pins within an assembly, which will lead to an underestimation of peak system temperature.

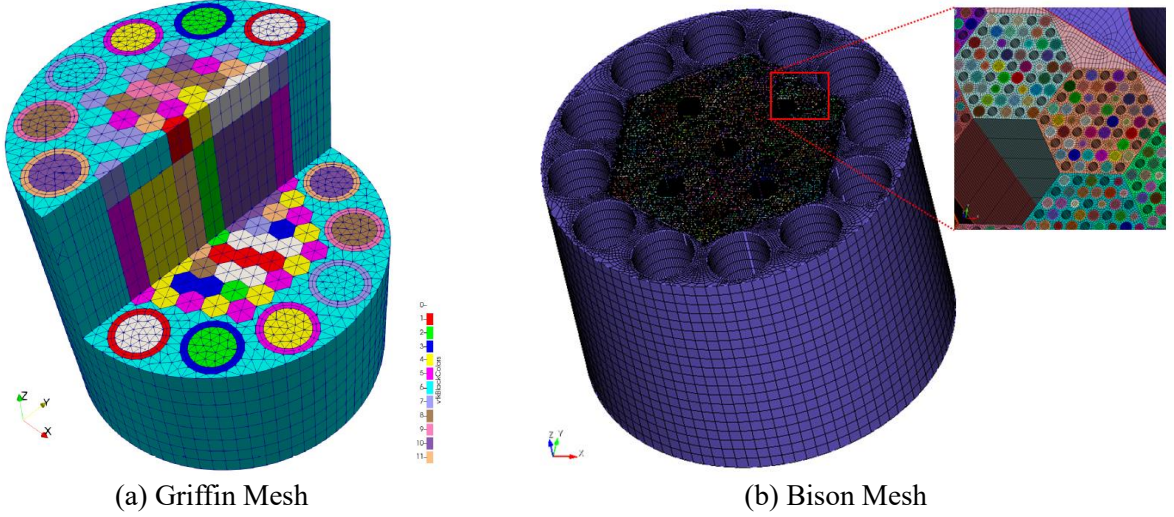


Figure 2. DireWolf Mesh

3. INADVERTENT CONTROL DRUM ROTATION (IDR)

3.1. Description of Transient

This transient scenario models the simultaneous rotation, at a constant speed, of all control drums from their critical position outward, which inserts positive reactivity into the core. The maximum drum rotation occurs at 2 seconds and is immediately followed by a constant-speed rotation inward to All Drums In (ADI) or shutdown configuration. The ejection and insertion speed are equal. Four different drum rotation speeds (0.5, 1, 2, and 3 degrees per second) are analyzed to determine the limiting speed, evaluated by reactivity insertion exceeding \$1.0 or violation of fuel maximum temperature ($>1600\text{ }^{\circ}\text{C}$) [9]. The total time modeled for this transient is 50 seconds; step size is 0.01s for $t \leq 2\text{s}$, 0.05s for $t \leq 3\text{s}$, 0.1s for $t \leq 4\text{s}$, 0.5s for $t \leq 5\text{s}$, and 1.0s for $t > 5\text{s}$. Figure 3 presents the drum position as function of time for all four cases. Note that a time convergence study is necessary to ensure physics are adequately captured.

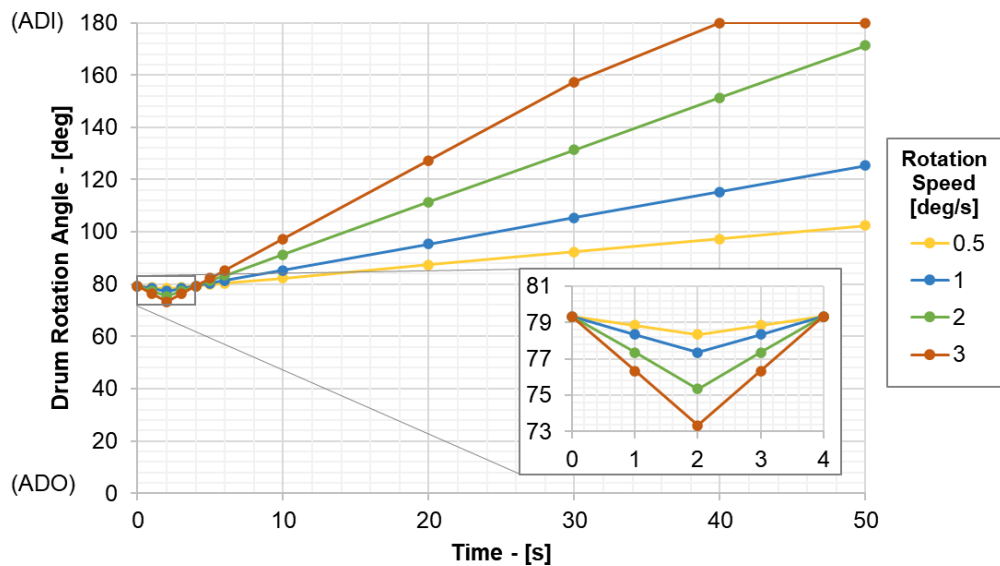


Figure 3. IDR – Drum Rotation versus Time

3.2. Results & Analysis

Figure 4 shows the core total power (solid lines) and reactivity (dashed lines) as a function of time for all cases. This figure shows that there is a significant difference in maximum power between the 0.5 and 1.0 deg/s cases, which remain below 4-times nominal core power, and 2.0 to 3.0 deg/s cases, which are nearly 40- and 840-times nominal power. It is also interesting to note that the peak power occurs after maximum rotation angle of drums (occurring at 2 seconds) for all cases other than 3.0 deg/s. The significantly larger maximum core power and early power peak of the 3.0 deg/s case is because this case goes prompt critical. Additionally, this early power peak is turned around with the Doppler feedback before the reactor trip at 2 seconds.

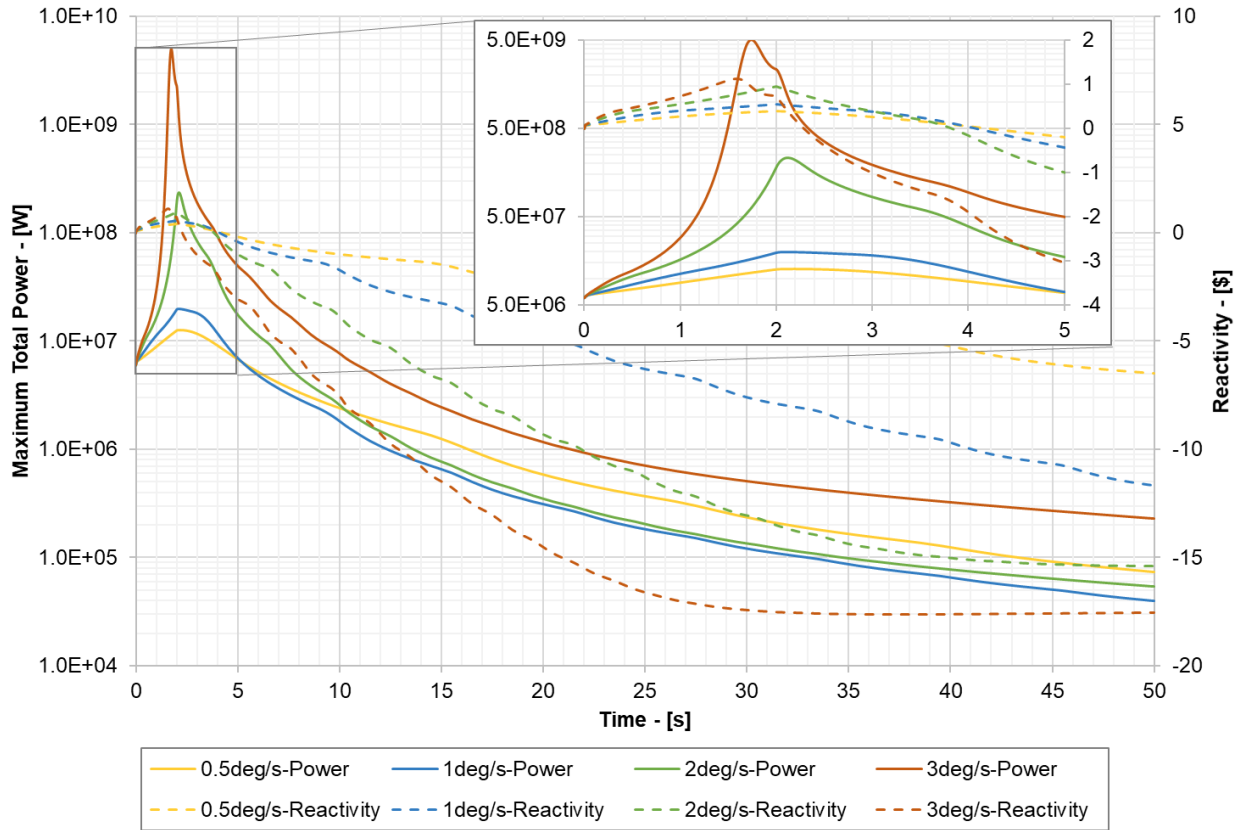


Figure 4. IDR – Total Power (solid lines) and Reactivity (dashed lines) versus Time

Table I shows the numerical maximums for all quantities presented in Figure 4. This table clearly shows that the 2 deg/s case is the limiting speed of the cases analyzed. The maximum component temperatures are within design limits, most notably the maximum fuel temperature (1050°C) is well below the limit of 1600°C . Again, note that maximum temperatures may be underestimated due to lack of pin-power reconstruction in this model. Figure 5 shows the component temperature evolution. The fuel peaks first at around 3 seconds, followed by the monolith, and then moderator. All core materials (other than the reflector) come to a uniform temperature around 26 seconds.

Table I. IDR – Maximum Power, Reactivity, and Component Temperatures

Rotation Speed [deg/s]	Maximum Core Power [MW]	Maximum Reactivity [\$]	Maximum Temperature [°C]				
			Fuel	Heat Pipe	Moderator	Monolith	Reflector
0.5	13	0.40	959.4	929.9	947.7	954.7	847.8
1	20	0.55	965.8	933.4	950.0	959.7	848.2
2	234	0.95	1050.1	988.3	986.3	1027.2	855.4
3	5025	1.13	2083.6	1527.8	1443.0	1703.0	945.6

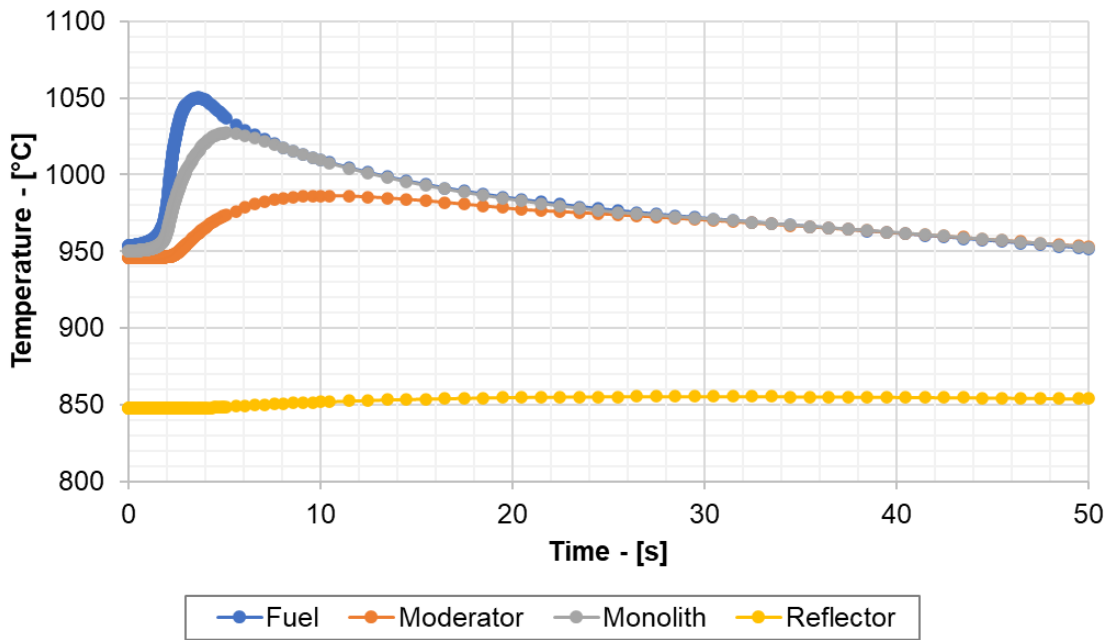


Figure 5. IDR (2 deg/s) – Component Maximum Temperature versus Time

Figure 6 presents the fast and thermal flux distributions, for the 2 deg/s case, at the time of maximum core power (2.12 seconds). The fast flux, Figure 6a, shows the expected peaking in the fuel. The thermal flux, Figure 6b, shows strong peaks in the reflector segments of the control drums. Figure 7 shows the power distribution at the time of maximum core power and the temperature distribution at the time fuel temperature peaks (3.66 seconds). The power distribution, Figure 7a, shows similar behavior to the fast flux, radially uniform peaking in the fuel. The temperature distribution, Figure 7b, show some radial hot spots (consistent with steady-state results), with the maximum fuel temperature occurring in center of the core. These distributions are uniform in the radial direction, as expected with the uniform rotation of all control drums.

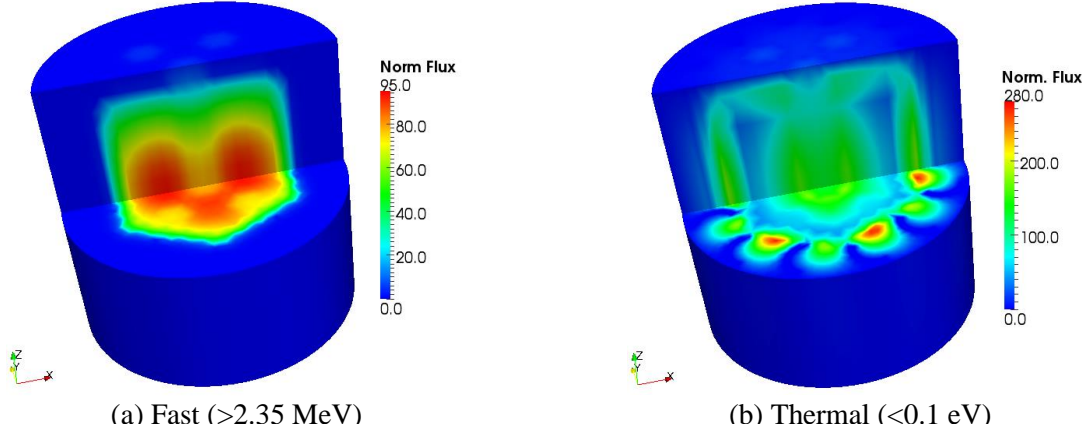


Figure 6. IDR (2 deg/s) – Fast and Thermal Flux Distribution at Time of Maximum Power (2.12 s).

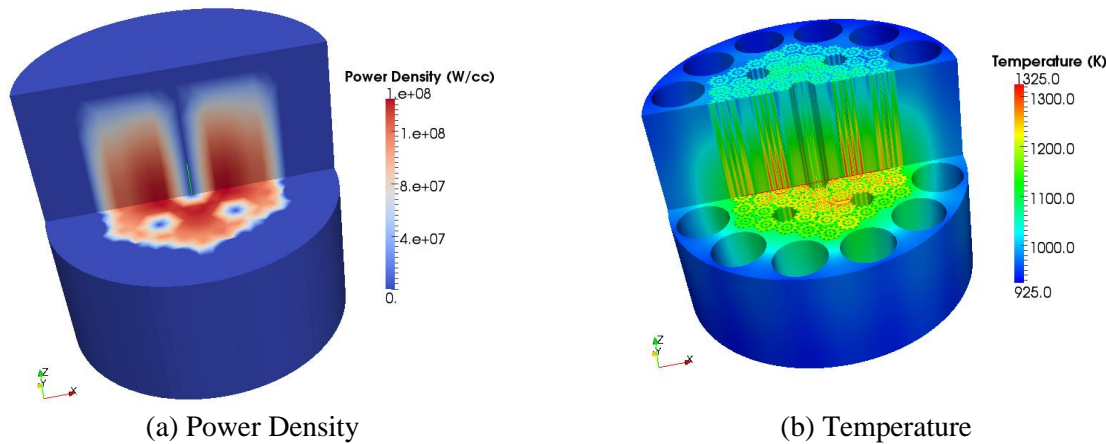


Figure 7. IDR (2 deg/s) – Power Density and Temperature Distribution at Time of Maximum Power (2.012 seconds) and Maximum Fuel Temperature (3.66 seconds).

4. SINGLE CONTROL DRUM ROTATION (SDR)

4.1. Description of Transient

This transient scenario models the sudden rotation of a single control drum from critical position to completely outward at a near constant speed. At the 2 second mark, all control drums are moved at a near constant speed to their shutdown configuration (ADI), aside from the drum immediately adjacent to the failed drum which is assumed to be stuck at the critical position. This transient is modeled for a total of 30 seconds. Four different drum rotation speeds (5, 10, 15, and 20 degrees per second) are analyzed to determine the limiting speed, evaluated by the core going prompt critical (reactivity > 1.0\$) or violation of fuel maximum temperature ($>1600^{\circ}\text{C}$). Step sizes for this transient are 0.01s for $t \leq 2\text{s}$, 0.05s for $t \leq 3\text{s}$, 0.1s for $t \leq 4\text{s}$, 0.5s for $t \leq 5\text{s}$, and 1.0s for $t > 5\text{s}$. Figure 8 shows the drum positions as a function of time for the failed, stuck, and all other drums. Again, note that a time convergence study is necessary to ensure physics are adequately captured.

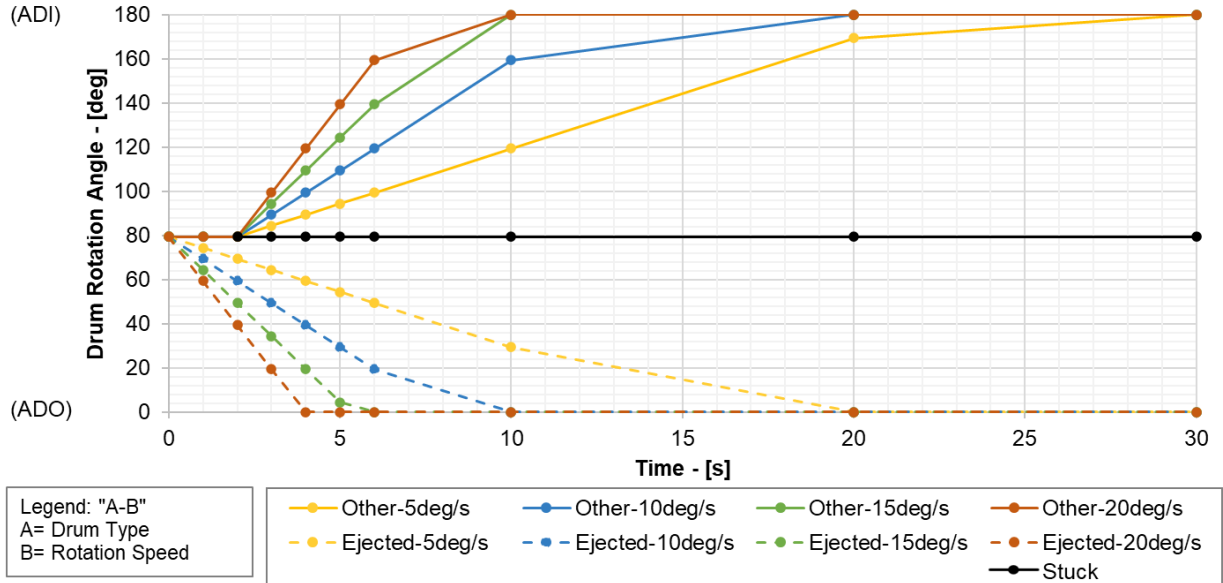


Figure 8. SDR – Rotation Angle versus Time

4.2. Results & Analysis

Figure 9 shows the core total power (solid lines) and reactivity (dashed lines) as a function of time for all cases. This figure shows the first two cases (5 and 10 deg/s) power remains below 5-times the nominal core power, for the 15 deg/s case it increases to about 20-times and the 20 deg/s case is over 200-times nominal power. The maximum power values occur at 2s (the point at which other drums are inserted to shut down the reactor), except for the 20 deg/s case which occurs slightly before this point – which is again because this scenario reaches prompt criticality.

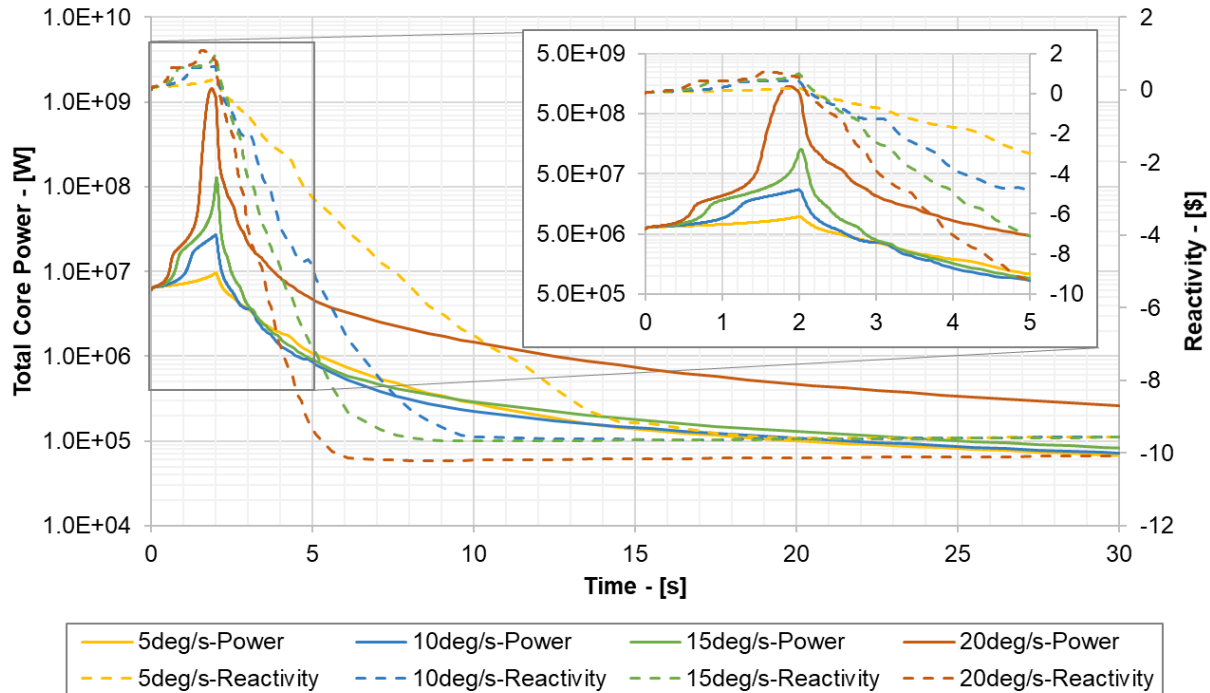


Figure 9. SDR – Total Power (solid lines) and Reactivity (dashed lines) versus Time

Table II shows the numerical maximums for all quantities presented in Figure 9. This table shows that the 15 deg/s case is the limiting speed of the cases analyzed. The maximum component temperatures are within design limits, most notably the maximum fuel temperature (976 °C) is well below the limit of 1600 °C. Figure 10 shows the component temperature evolution. The fuel peaks first at around 4 seconds, followed by the monolith, and then moderator. All core materials (other than the reflector) reach a uniform temperature around 14 seconds.

Table II. SDR – Maximum Power, Reactivity, and Component Temperatures

Rotation Speed [deg/s]	Maximum Core Power [MW]	Maximum Reactivity [\$]	Maximum Temperature [°C]				
			Fuel	Heat Pipe	Moderator	Monolith	Reflector
5	10	0.31	954.9	927.3	945.9	950.8	847.8
10	27	0.63	961.5	929.6	947.3	954.5	847.9
15	127	1.00	976.2	935.4	950.9	963.5	848.4
20	1428	1.09	1275.2	1071.1	1049.3	1138.0	872.0

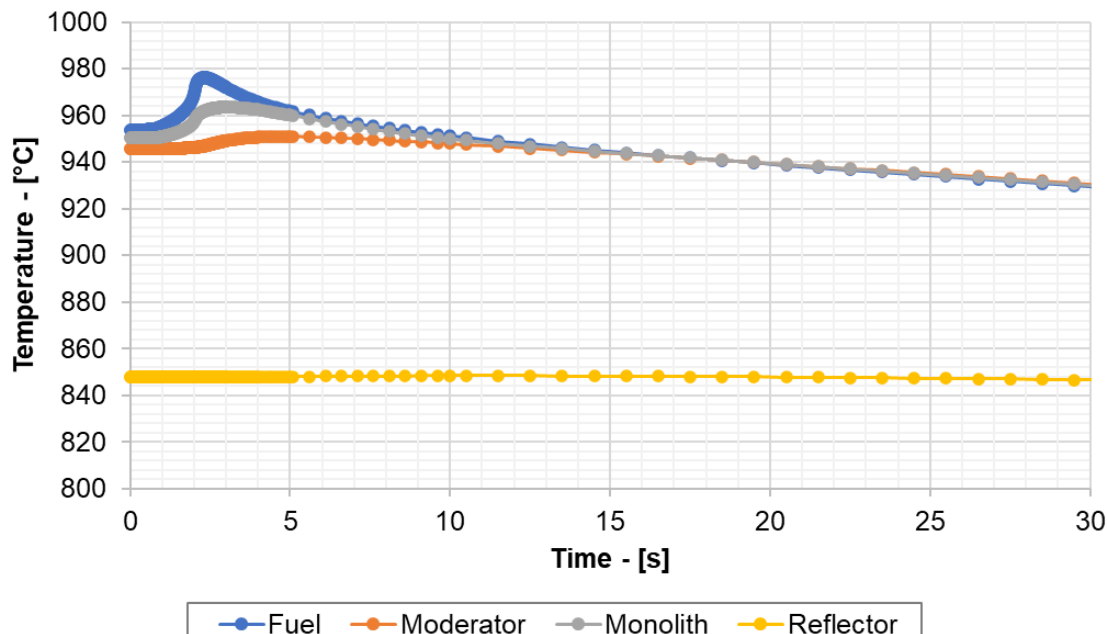


Figure 10. SDR (15 deg/s) – Component Maximum Temperature versus Time

Figure 11 presents the fast and thermal flux distributions, for the 15 deg/s case, at the time of maximum core power (2.02 seconds). The fast flux, Figure 11a, shows the expected peaking in the fuel with a tilt toward the right side of the core near the location of the failed drum. The thermal flux, Figure 11b, shows the expected peaks in the reflector region, with a severe spike at the location of the failed drum (on the right-hand side of the core). Figure 12 shows the power distribution at the time of maximum core power (2.02 seconds) and the temperature distribution at the time fuel temperature peaks (2.32 seconds). The power distribution, Figure 12a, shows similar behavior to the fast flux, peaking in the fuel near the failed drum. The temperature distribution, Figure 12b, shows some radial hot spots, with the maximum fuel temperature occurring toward the right side of the core.

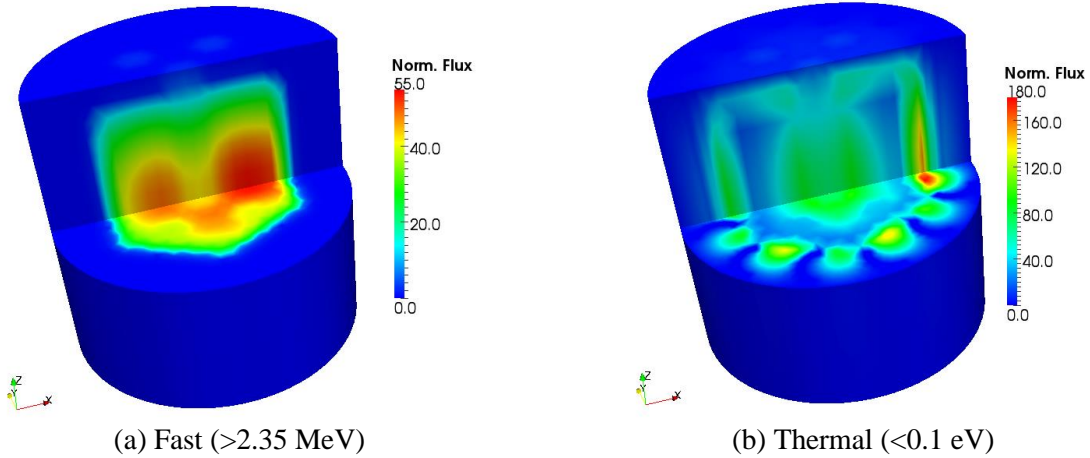


Figure 11. SDR (15 deg/s) – Fast and Thermal Flux Distribution at Time of Maximum Power (2.02 seconds).

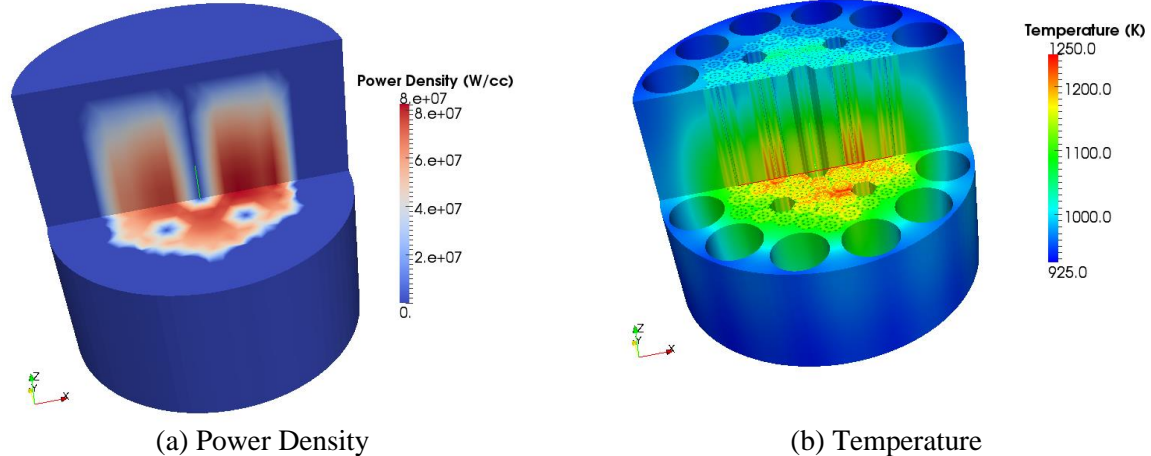


Figure 12. SDR (15 deg/s) – Power Density and Temperature Distribution at Time of Maximum Power (2.02 seconds) and Time of Maximum Fuel Temperature (2.32 seconds).

5. CONCLUSION

This paper has shown DireWolf's capability to model reactivity insertion transients of a heat pipe cooled micro-reactor. The inadvertent partial rotation of all control drums and the complete ejection of a single control drum are presented. Sensitivity studies were performed for each transient scenario to determine limiting rate of reactivity insertion. The evolution of the total core power and reactivity and component temperatures was shown as well as maximum values for the insertion rate sensitivity studies. 3D flux, power, and temperature distributions are also presented for the limiting cases. Qualitatively the results are as expected, the single drum rotation case produced an asymmetric radial power distribution while the inadvertent rotation of all control drums showed a symmetric distribution. The determination of a limiting inadvertent drum rotation speed of 2 deg/s aligns with previous analysis performed with GOTHIC [10]. This is important because it provides confirmation that the less-accurate coarse-mesh tool GOTHIC maybe capable of accurately predicting bounding transient events. Future studies are necessary to confirm the results of these analyses, with specific attention paid to pin-power reconstruction, time convergence, and large spacing of temperature intervals in the cross-section library.

ACKNOWLEDGMENTS

This work was supported by the DOE ARPA-E MEITNER award (DE-FOA-0001798). This research made use of the resources of the High-Performance Computing Center at Idaho National Laboratory, which is supported by the Office of Nuclear Energy of the U.S. Department of Energy and the Nuclear Science User Facilities under Contract No. DEAC07-05ID14517.

REFERENCES

1. C. Matthews, et al., "Coupled multiphysics simulations of heat pipe microreactors using DireWolf." *Nuclear Technology*, **207**(7), pp. 1142-1162 (2021).
2. Y. Wang, et al., "Rattlesnake: A MOOSE-Based Multiphysics, Multischeme Radiation Transport Application," *Nuclear Technology*, **207**(7), pp. 1047-1072 (2021).
3. R L Williamson, et al., "Multidimensional multiphysics simulation of nuclear fuel behavior," *Journal of Nuclear Materials*, **423**, pp. 149–163 (2012).
4. J. E. Hansel, et al., "Sockeye Theory Manual," Research Report INL/EXT-19-54395, Idaho National Laboratory, https://inldigitallibrary.inl.gov/sites/sti/sti/Sort_27069.pdf (2020).
5. Roskoff, et al., "Modeling and Analysis of a Micro-reactor using the DireWolf Code Suite," *Proceedings of PHYSOR 2022: Making Virtual a Reality*, (2022), submitted.
6. J. Ortensi, et al., "A Newton Solution for the Superhomogenization Method: The PJFNK-SPH," *Annals of Nuclear Energy*, **111**, pp. 579-594 (2018).
7. V. Labouré, et. al., "Hybrid super homogenization and discontinuity factor method for continuous finite element diffusion", *Annals of Nuclear Energy*, **128**, pp. 443-454 (2019).
8. S. Schunert, et. al., "Control rod treatment for FEM based radiation transport methods", *Annals of Nuclear Energy*, **127**, pp. 293-302 (2019).
9. "Topical Report on Uranium Oxycarbide (UCO) Tristructural Isotropic (TRISO) Coated Particle Fuel Performance: Topical Report EPRI-AR-1(NP)," EPRI, Palo Alto, CA (2019).
10. "GOTHIC Containment Analysis Package Technical Manual, Version 7.2," NAI 8907-06, Rev. 15, EPRI, Palo Alto, CA (2004).